Installation damage testing

CONTROL:

Specimen No.	Peak Load (N)	Peak Load (kN/m)
1	19752	109.7
2	20884	116.0
3	18839	104.7
4	18972	105.4
5	20067	111.5
6	19243	106.9
Mean	**19626**	**109.0**
Std. Dev.	**773**	
Coef. of Var.	**3.94**	

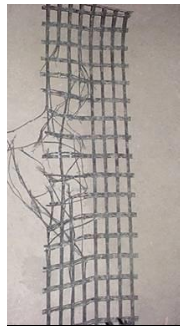

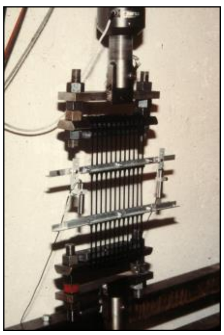

EXHUMED: <150 mm crushed stone

Specimen No.	Peak Load (N)	Peak Load (kN/m)
1	17813	99.0
2	17776	98.8
3	17078	94.9
4	17040	94.7
5	16922	94.0
6	18738	104.1
7	18823	104.6
8	17030	94.6
9	18217	101.2
Mean	**17715**	**98.4**
Std. Dev.	**750**	
Coef. of Var.	**4.23**	

$FS_{ID} = 109.0/98.4 = \underline{1.11}$

r.j. bathurst 93

Constant load creep testing

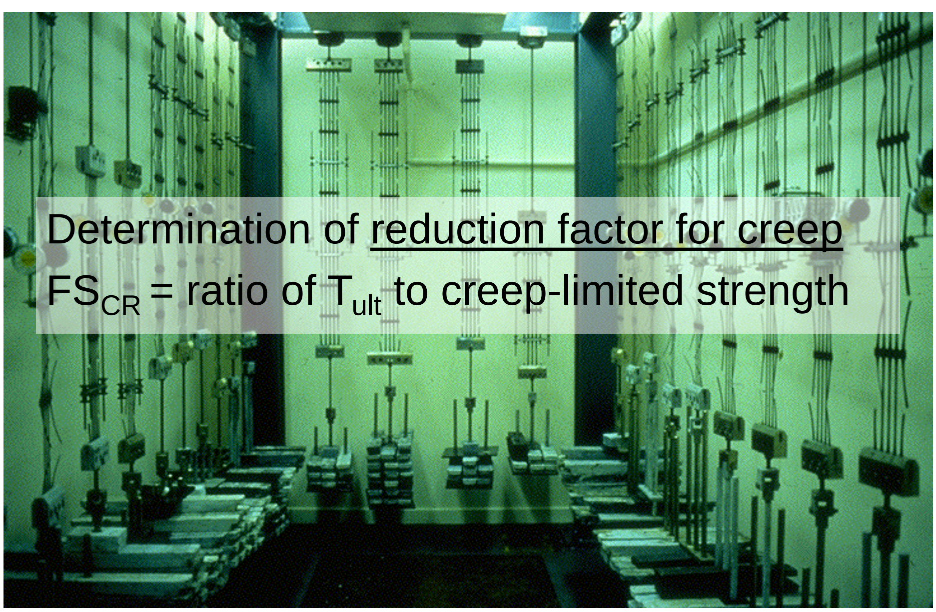

r.j. bathurst 94

Creep reduction factor

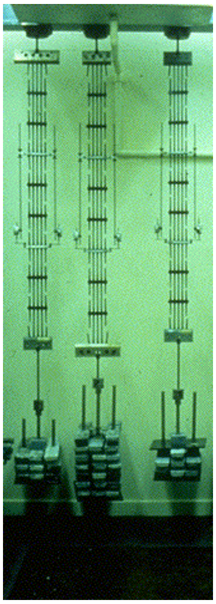

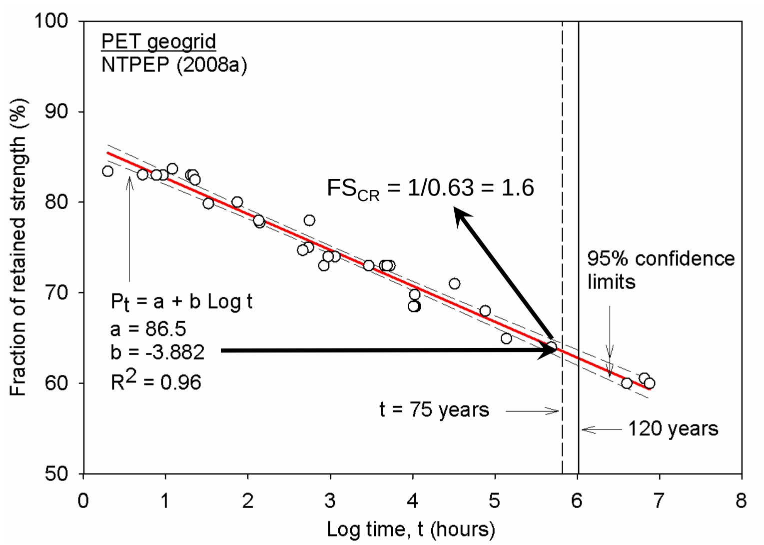

Bathurst, R.J., Huang, B. and Allen, T.M. 2012. Interpretation of laboratory creep testing for reliability-based analysis and load and resistance factor design (LRFD) calibration, Geosynthetics International, Vol. 19, No. 1, pp. 39-53

Summary of creep testing database and computed creep reduction factors (FS_{CR})

Data group	Reinforcement material	Number of different products	Range of (kN/m) (b)	Number of creep-rupture data points	Test method	Range of creep rupture time (e) (log hours)	FS_{CR} (i) 75 years (5.82 log hours)	FS_{CR} (i) 120 years (6.02 log hours)	Reference
1	PET geogrid	5	52.8 – 435	39	Block (c) SIM (d)	0.30 – 6.88	1.56	1.58	NTPEP (2008a)
2	PET geogrid	3	60.4 – 471	24	Block SIM	0.84 – 6.64	1.41	1.43	NTPEP (2008b)
3	PET geogrid	3	35.7 – 427	19	Block SIM	-0.34 – 6.21	1.56	1.58	NTPEP (2009a)
4	PET geogrid	3	37.5 – 190.5	19	Block SIM	-0.25 – 6.53	1.52	1.54	NTPEP (2009b)
5	PET geogrid	5	154 – 414	21	Block SIM	-0.37 – 6.21	1.59	1.61	NTPEP (2009c)
6	PET geogrid	15	42.7 – 230	20	Block SIM	0.35 – 6.99	1.39	1.40	NTPEP (2010a)
7	PET geogrid	7	32.8 – 174	20	Block SIM	0.34 – 6.85	1.49	1.51	NTPEP (2010b)
8	PET geogrid	1	75	10	Block	-1.24 – 6.65	1.67	1.70	Thornton and Arnett (1997a)
9	PET geogrid	1	121	11	Block	-0.72 – 6.76	1.64	1.65	Thornton and Arnett (1997b)
10	PET geogrid	1	3.5 (kN/rib)	23	Block SIM	0.89 – 6.38	1.48	1.49	Thornton et al. (1998a)
11		1	NA(g)	20	Block SIM	-0.52 – 6.08	1.57	1.58	
12	PET geogrid	1	104.9	12	SIM	-0.78 – 10.15	1.45	1.46	Greenwood and Voskamp (2000)
13	PET strap	1	325	22	Conventional SIM	1.32 – 6.89	1.43	1.44	Greenwood et al. (2004)
14	PET strap	20	99.9 – 1480	27	Block SIM	0.51 – 7.68	1.36	1.36	NTPEP (2010a)
15	PET yarn	1	NA(g)	12	Block SIM	-0.90 – 6.51	1.47	1.48	Thornton et al. (1998b)
16	PET yarn (a)	1	42.1	12	SIM	-0.60 – 6.51	1.66	1.67	Greenwood (2002)
17	PET yarn	6	NA	27	Block SIM	-1.74 – 6.96	1.59	1.60	Stevenson and Lozano (2004)
18	PET nonwoven geotextile	1	11.0	13	SIM	-1.82 – 6.99	1.46	1.47	Bueno et al. (2005)
19	PP nonwoven geotextile	1	11.1	12	SIM	-1.71 – 3.69	1.76	1.78	
20	PP woven geotextile	1	52	24	Conventional SIM	-0.43 – 8.18	2.80	2.89	Thornton and Baker (2002)
21	HDPE geogrid	3	61.9 – 122.5	14	Block	-0.19 – 4.44	3.12	3.20	Small and Greenwood (1992)
22	HDPE geogrid	4	73 – 185	62	SIM	0.00 – 7.44	2.48	2.51	Wrigley et al. (2004)
23	HDPE geogrid	5	NA(g)	39	Block	-1.79 – 8.50	NA(g)	NA(g)	Wrigley et al. (1999)
24	HDPE geogrid	3	75.2 – 149	27	Block SIM	0.45 – 5.91	2.54	2.57	NTPEP (2010c)
25		1	180	11		2.65 – 6.27	2.59	2.65	
		∑ = 94		∑ = 540			1.36 – 3.12	1.36 – 3.20	

Bathurst, R.J., Huang, B. and Allen, T.M. 2012. Interpretation of laboratory creep testing for reliability-based analysis and load and resistance factor design (LRFD) calibration, Geosynthetics International, Vol. 19, No. 1, pp. 39-53

Geosynthetics Specifier's Guide

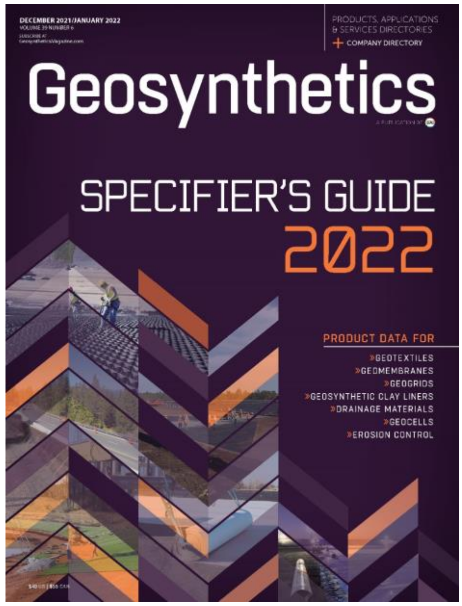

r.j. bathurst https://geosyntheticsmagazine.com/specifiers-guide/ 97

Geosynthetics Specifier's Guide

| Geogrids |

Product Name	Manufacturing Process	Polymer Type [1]	Coating Type [1]	Dimensional Properties [2]			Tensile Strength/[Elongation] ASTM D 6637 [2] kN/m (lb/ft)/%				Creep Limited Strength-MD [3] ASTM D 5262 kN/m (lb/ft)	LTDS GRI GG4-MD [4] kN/m (lb/ft) (in sand)	Manufacturer's Suggested Applica-tions [5]
				Mass/Unit Area ASTM D 5261 g/m2 (oz/yd2)	Aperture Size mm (in)		Strength @ 5% Strain		Ultimate Strength/% (Tult)				
					MD	XD	MD	XD	MD	XD			
Mirafi (TenCate Geosynthetics)													**www.mirafi.com**
Miragrid 2XT	woven	PET	PVC	NP	22 (0.875)	25 (1.0)	NA	NA	29.2 (2000)	29.2 (2000)	18.2 (1250)	15.8 (1082)	W, S, E
Miragrid 3XT	woven	PET	PVC	NP	22 (0.875)	25 (1.0)	15.4 (1056)	NA	46.0 (3150)	NA	28.7 (1969)	24.9 (1705)	W, S, E
Miragrid 5XT	woven	PET	PVC	NP	22 (0.875)	25 (1.0)	25.4 (1740)	NA	62.7 (4300)	NA	39.2 (2688)	34.0 (2327)	W, S, E
Miragrid 7XT	woven	PET	PVC	NP	22 (0.875)	25 (1.0)	31.5 (2160)	NA	83.2 (5700)	NA	52.0 (3563)	45.0 (3084)	W, S, E
Miragrid 8XT	woven	PET	PVC	NP	22 (0.875)	25 (1.0)	36.8 (2520)	NA	102.1 (7000)	NA	63.8 (4375)	55.3 (3788)	W, S, E
Miragrid 10XT	woven	PET	PVC	NP	22 (0.875)	25 (1.0)	45.5 (3120)	NA	138.6 (9500)	NA	86.6 (5938)	75.0 (5141)	W, S, E
Miragrid 20XT	woven	PET	PVC	NP	38 (1.5)	18 (0.7)	77.9 (5340)	NA	181.2 (12,420)	NA	105.4 (7221)	91.2 (6252)	W, S, E
Miragrid 22XT	woven	PET	PVC	NP	81 (3.2)	7.6 (0.3)	97.8 (6700)	NA	259.1 (17,760)	NA	150.7 (10,326)	130.4 (8940)	W, S, E

r.j. bathurst 98

Internal and connection failure modes

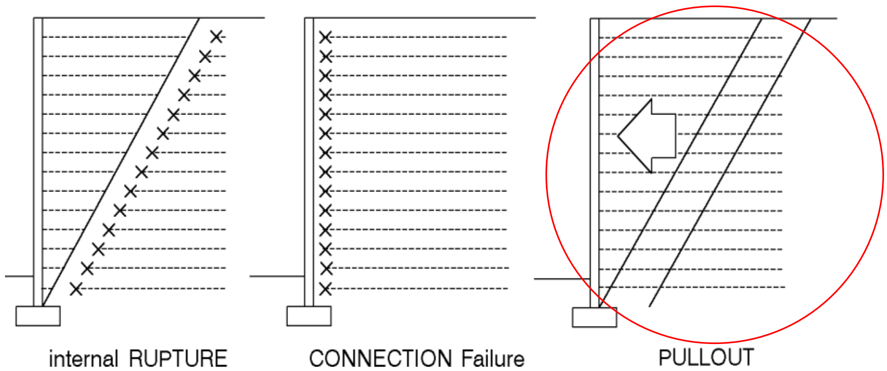

r.j. bathurst

99

Pullout test box

100

Pullout test box

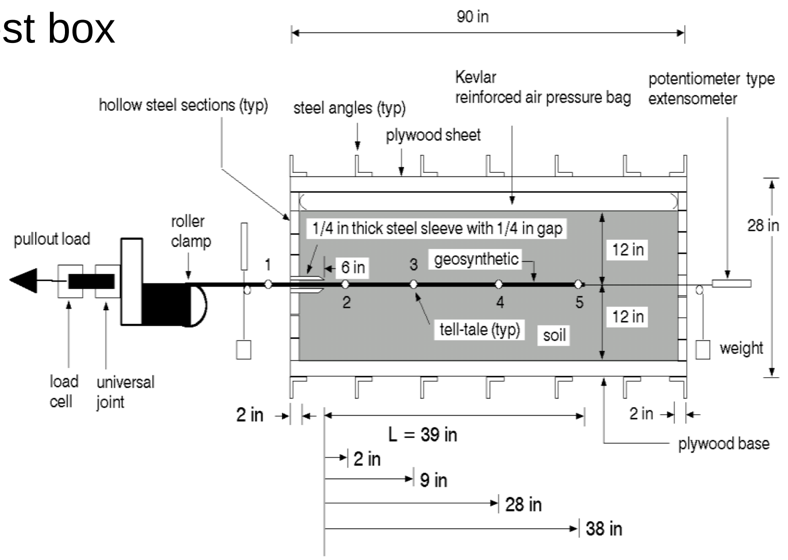

Note: Inside width of box = 30 in

Figure A: Cross-section view of pullout box apparatus and general arrangement of geosynthetic test specimen.

Pullout testing

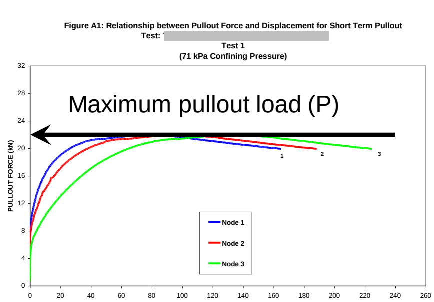

Pullout testing

$P = 2 \times L \times W \times \sigma_n \times C_i \times \tan \phi$

$C_i = P / (2 \times L \times W \times \sigma_n \times \tan \phi)$

where:

- P = pullout load (kN)
- L = length of specimen (m)
- W = width of specimen (m)
- σ_n = normal stress (kPa)
- ϕ = soil friction angle (degrees)
- C_i = coefficient of interaction (0.70 to 1.0)

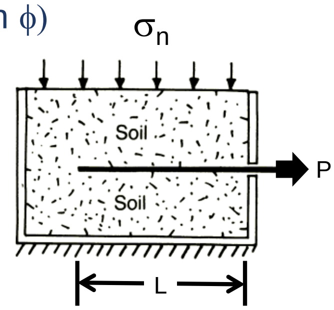

r.j. bathurst
103

Internal and connection failure modes

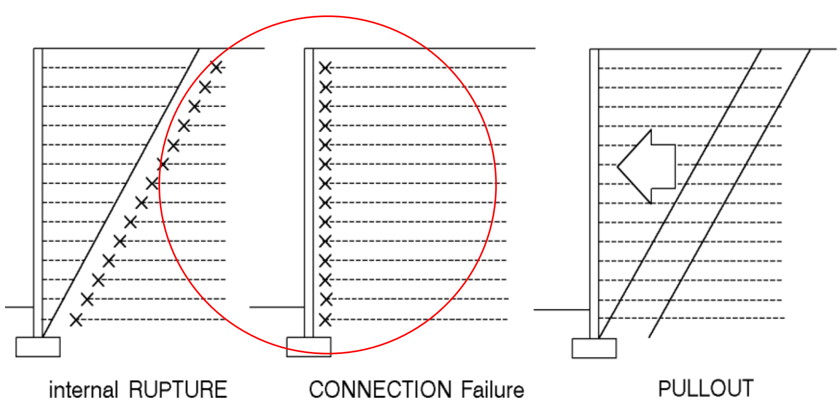

r.j. bathurst
104

Connections

r.j. bathurst

105

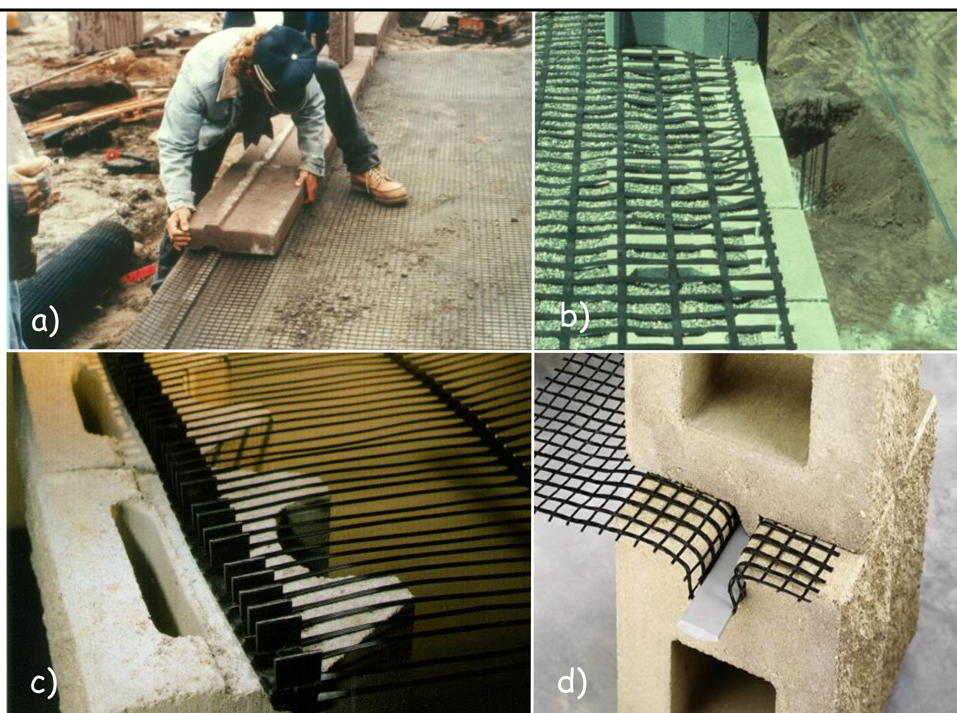

r.j. bathurst

106

Connection testing

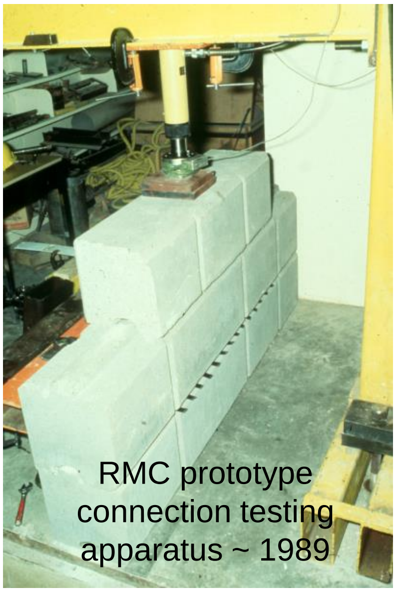

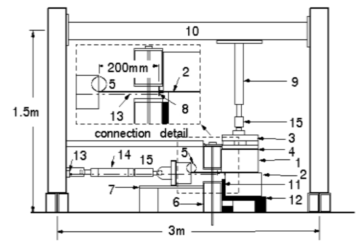

r.j. bathurst 107

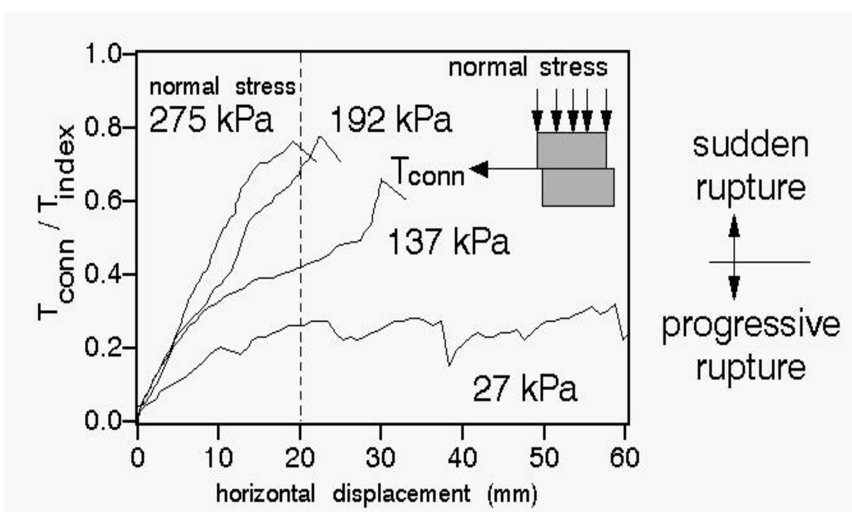

r.j. bathurst 108

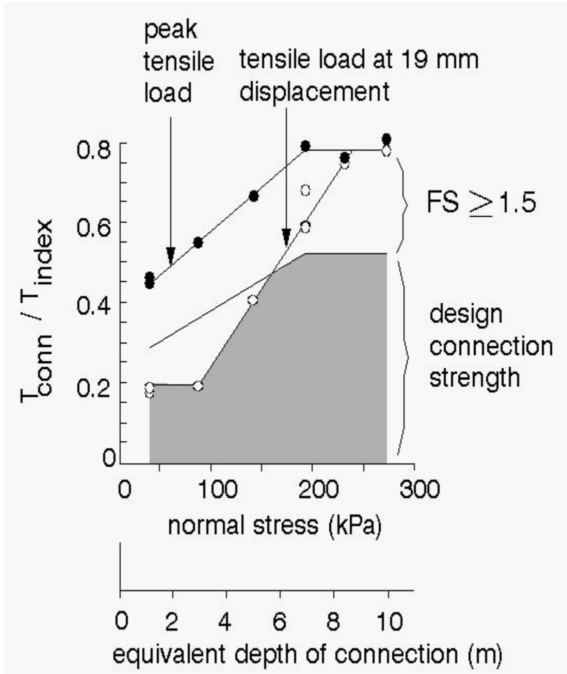

r.j. bathurst 109

Royal Roads modular block wall (Victoria, BC, Canada)

r.j. bathurst 110

Royal Roads modular block wall

r.j. bathurst
111

Connection testing

r.j. bathurst
112

Probabilistic (reliability-based) internal stability analysis and design of reinforced soil walls

r.j. bathurst

113

Reliability-based design gives a more nuanced appreciation of the margin of safety for internal limit states for MSE walls compared to conventional factor of safety, partial factor, and load and resistance factor design (LRFD) approaches

r.j. bathurst

114

Performance function for each limit state

Nominal factor of safety

$$F_n = \frac{R_n}{Q_n}$$

λ_R = ratio of measured resistance to predicted (nominal) resistance

nominal resistance (pullout capacity)

$$g = \frac{\lambda_R R_n}{\lambda_Q Q_n} - 1$$

nominal (tensile) load

λ_Q = ratio of measured load to predicted (nominal) load

$$Q_n = T_{max} = S_v K_r \sigma_v z$$

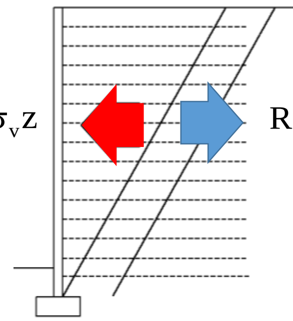

$$R_n = P_c = 2f^* L_e \sigma_v R_c$$

Pullout limit state

r.j. bathurst 115

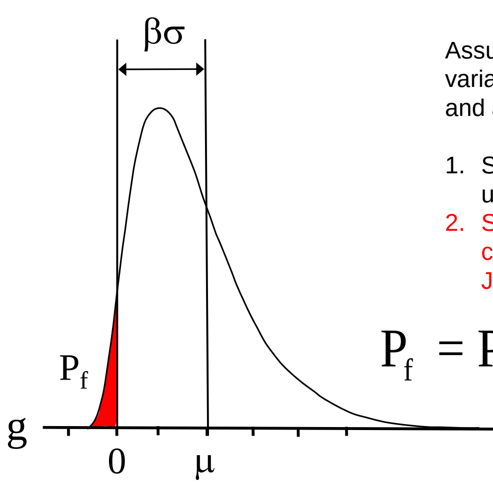

Assume λ_R, λ_Q, R_n and Q_n are random variables described by mean and COV, and are lognormally distributed

1. Solve for P_f (probability of failure) using Monte Carlo simulation, or
2. Solve for β (reliability index) using closed-form solution of Bathurst and Javankhoshdel (2017)

$$P_f = P(g < 0) = 1 - \Phi(\beta)$$

Standard normal cumulative distribution function NORMSDIST in EXCEL

$$g = \frac{\lambda_R R_n}{\lambda_Q Q_n} - 1$$

r.j. bathurst 116

Nominal factor of safety

$$F_n = \frac{R_n}{Q_n}$$

Non-dimensional functions of lognormally distributed random variables λ_R, λ_Q, R_n and Q_n described by mean and COV

$$\beta = A + B \times \mathrm{Ln}(F_n)$$

r.j. bathurst 117

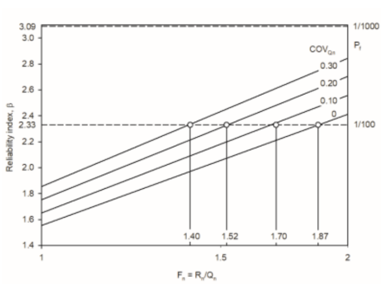

a) LM1-TM (AASHTO 2017)

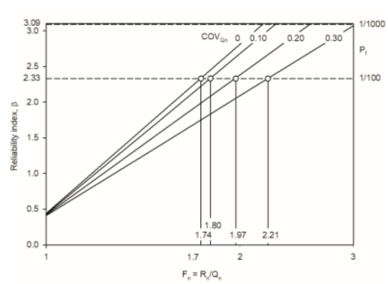

b) LM2-TM (AASHTO 2020)

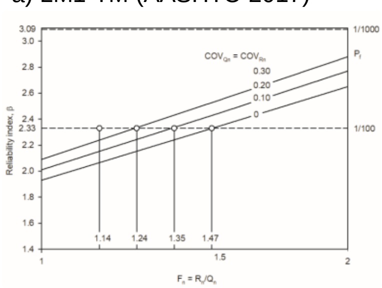

c) LM1-PM1 (AASHTO 2017)

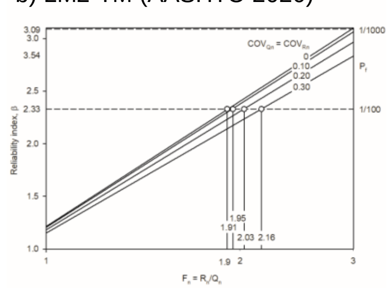

d) LM2-PM1(AASHTO 2020)

Figure 3. Reliability index versus ratio of nominal resistance to nominal load

r.j. bathurst 118

Conclusions

- Reliability-based design gives a more nuanced appreciation of the margin of safety for internal limit states for MSE walls compared to conventional factor of safety, partial factor, and load and resistance factor design (LRFD) approaches
- Accuracy of the load and resistance models *and* uncertainty in the magnitude of nominal load and resistance terms is considered explicitly
- The calculation of reliability index can be done using a spreadsheet and thus Monte Carlo simulation is avoided
- The method provides a quantitative link between the conventional factor of safety familiar to geotechnical engineers, and reliability index which is used in contemporary probabilistic analysis and design of geotechnical structures

r.j. bathurst 119

SELECTED REFERENCES

Bathurst, R.J. and Allen, T.M. 2021. Reliability assessment of internal stability limit states for two as-built geosynthetic MSE walls. ISSMGE International Journal of Geoengineering Case Histories 6(4): 67-84 (https://doi.org/10.4417/IJGCH-06-04-05).

Bathurst, R.J., Miyata, Y. and Allen, T.M. 2020. Deterministic and probabilistic assessment of margins of safety for internal stability of as-built PET strap reinforced soil walls. Geotextiles and Geomembranes 48: 780-792 (https://doi.org/10.1016/j.geotexmem.2020.06.001).

Bathurst, R.J., Allen, T.M., Miyata, Y., Javankhoshdel, S. and Bozorgzadeh, N. 2019. Performance-based analysis and design for internal stability of MSE walls. Georisk 13(3): 214-225 (https://doi.org/10.1080/17499518.2019.1602879).

Bathurst, R.J., Lin, P. and Allen, T.M. 2019. Reliability-based design of internal limit states for mechanically stabilized earth walls using geosynthetic reinforcement. Canadian Geotechnical Journal 56(6): 774-788 (https://doi.org/10.1139/cgj-2018-0074).

Bathurst, R.J. and Javankhoshdel, S. 2017. Influence of model type, bias and input parameter variability on reliability analysis for simple limit states in soil-structure interaction problems. Georisk 11(1): 42-54 (http://dx.doi.org/10.1080/17499518.2016.1154160).

r.j. bathurst 120